The effect of a solar flare on chromospheric oscillations

David C L Millar, Lyndsay Fletcher & Ryan O Milligan

THE CARNEGIE TRUST FOR THE UNIVERSITIES OF SCOTLAND

University of Glasgow

Background

The chromosphere has a ≈3 minute oscillatory signature, caused by the **acoustic cut-off frequency ω_c** of the stratified medium. In regions with high magnetic fields, disturbances travel up from the photosphere along field lines as magnetoacoustic gravity (MAG) waves.

$$\omega_c = \frac{\gamma g \cos\theta}{2c_s} \propto \frac{g\cos\theta}{\sqrt{T}}$$

γ = ratio of specific heats
c_s = sound speed
g = gravitational acceleration
T = temperature
θ = angle between ***g*** and ***B*** fields

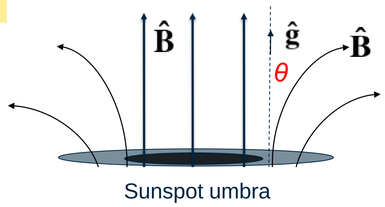

Flare and datasets

M1.1 flare – 20140906T1709 – observed with CRISP at the SST in H-alpha and Calcium II 8542 (Figure 1). Additional analysis was performed using AIA 1600 and 1700 filters, and HMI vector magnetograms. Intensity oscillations were analysed from groups of pixels across the field of view and at different wavelength steps, in **pre-flare** and **post-impulsive** time periods (Figure 2).

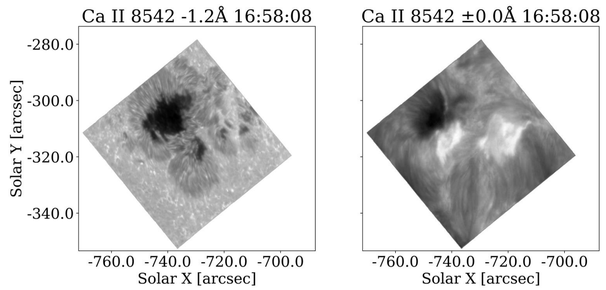

Figure 1: Images from the Calcium II 8542 wing (left) and core(right), at the time of the flare onset, showing the photosphere and chromosphere, respectively.

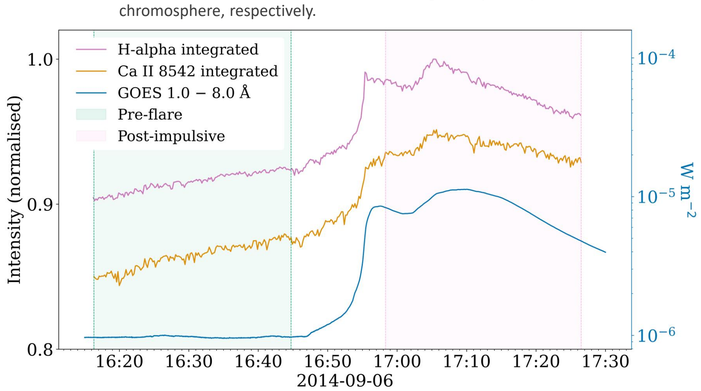

Figure 2: Lightcurves from GOES and integrated CRISP intensity. The shaded areas indicate the pre-flare and post-impulsive time periods.

Methodology

To identify clear oscillatory signals, the power spectra for each timeseries were fitted to one of three models (M1, M2 and M3, Figure 3). This method is similar to [1], [2].

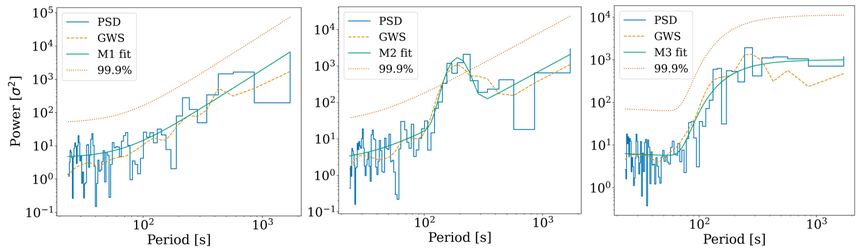

Figure 3: Examples of the three spectrum models used to identify oscillations. Left to right: M1 (red noise), M2 (red noise with a Gaussian bump), M3 (red noise with a kappa function).

Oscillatory signals are identified by a pronounced bump in the spectrum, modeled by a Gaussian (M2), the height of which is above a 99.9% confidence level. Spectra with no significant oscillations are fit to M1 (red noise) and M3 (red noise with kappa function to account for flattening at low frequencies).

Results – locations of signals

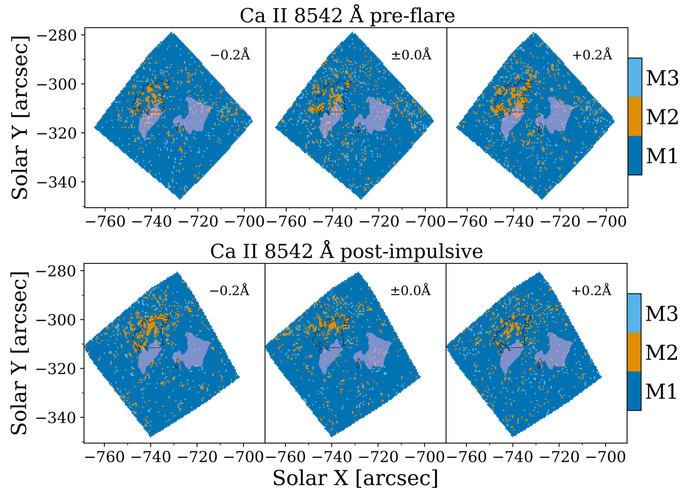

Figure 4: The spectrum model which was identified for each group of pixels at selected wavelengths for Calcium II 8542. The border of the sunspot umbra is shown by the black contour, and the shaded contours show the locations of the flare ribbons.

The locations of significant oscillatory behaviour (orange in figure 4) are different in the pre-flare and post-impulsive results. In pre-flare there are signals from all over the umbra, while post-impulsive shows a concentration of signals at the northern umbral border.
There are few signals from the locations of the flare ribbons, it seems the footprints have suppressed any present oscillations in the post-impulsive phase.

Results – typical periods of oscillation

Figure 5 shows the typical periods of the signals from pixels which matched M2. We can see that the periods increase as location moves away from the centre of the sunspot. It also seems that in positions with oscillations in both time periods, the post-impulsive periods tend to be greater than pre-flare.

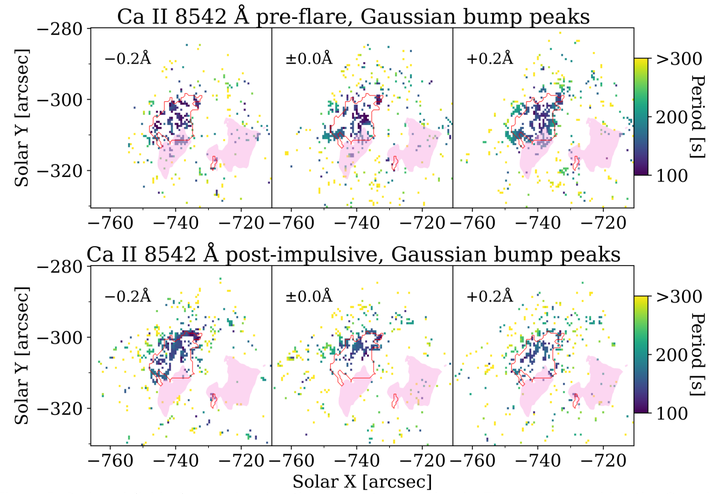

Figure 5: Reduced field of view showing the sunspot more closely. The period at which the Gaussian bumps in M2 pixels peak, for the pre-flare and post-impulsive periods. The red contour is the umbra border, and the shaded contour shows the flare ribbon locations.

Conclusions

The main results are thus:

- The locations of strong intensity oscillations change from pre-flare to post-impulsive
- The typical periods of these oscillations increase going from pre-flare to post-impulsive

Both of these phenomena can be explained by a change to the magnetic field inclination in the chromosphere caused by the flare activity. The MAG waves are guided by the field lines to different locations and the value of θ increases, reducing the cut-off frequency.

These results demonstrate one of the ways solar flares can affect active regions, and I plan to investigate this further with spectropolarimetric observations (to measure magnetic field) and MHD simulations (using Lare2d).

This poster presents a selection of the results from this study. For in depth analysis see Millar et al, 2021 [3].

References

[1] Inglis, A., Ireland, J. and Dominique, M., 2015. *ApJ*, 798(2), p.108.
[2] Auchère, F., Froment, C., Bocchialini, K., Buchlin, E. and Solomon, J., 2016. *ApJ*, 825(2), p.110.
[3] Millar, D., Fletcher, L. and Milligan, R., 2021. *MNRAS*, 503(2), pp.2444-2456.